mM NaCl, and 10 mM phenylmethylsulfonyl fluoride (PMSF)] was centrifuged at 30,000*g* for 20 min. To the supernatant (10 ml) was added 0.5 ml of 5% polyethyleneimine. After swirling on ice, the sample was centrifuged at 30,000*g* for 20 min. The proteins in the supernatant were precipitated with ammonium sulfate. Each TAF fragment was purified using SP Sepharose and Q Sepharose columns (Pharmacia) and characterized by electrospray ionization mass spectroscopy. NMR spectra of TAF_{1-140} alone showed unexpectedly broad peaks, presumably attributable to dimer formation of the histone homology region [X. Xie *et al.*, *Nature* **380**, 316 (1996); A. Hoffmann *et al.*, *ibid.*, p. 356]. This broadening made it impractical to pursue NMR studies of TAF_{1-140} alone.

9. The ability of the TAF fragments to bind to $VP16_C$ was estimated by GST pull-down assays. GST-$VP16_C$ beads (loaded with 200 μg of protein) were incubated with 50 μg of each TAF fragment in 200 μl of binding buffer [20 mM tris-HCl (pH 7.4), 50 mM NaCl, 2 mM dithiothreitol (DTT), 10 mM $MgCl_2$, 0.01% NP-40, and 10% glycerol] at 4°C for 1 hour, and then washed five times with 200 μl of the same buffer. The samples were dissolved in SDS–polyacrylamide gel electrophoresis (PAGE) loading buffer and analyzed by SDS-PAGE.
10. The DNA encoding $VP16_C$ was generated as a Bam HI–Eco RI DNA fragment with PCR and cloned into the *E. coli* vector pGEX3X. Expression of the construct in *E. coli* yielded a GST-$VP16_C$ fusion protein. The fusion protein was purified on a glutathione-Sepharose affinity column and cleaved with factor Xa. The cleavage mixture was purified by glutathione-Sepharose affinity chromatography. This procedure resulted in a protein with three NH_2-terminal residues (Gly-Ile-Pro) derived from the construct, followed by residues 452 to 490 of VP16. Uniformly (>95%) labeled proteins with ^{15}N or with ^{15}N and ^{13}C were obtained by growing the bacteria in minimal medium supplemented with either $^{15}NH_4Cl$ or both $^{15}NH_4Cl$ and [^{13}C]glucose as the sole nitrogen and carbon sources. The labeled proteins were dissolved to 0.5 to 0.9 mM in either 95% H_2O plus 5% ^2H_2O or 99.96% ^2H_2O containing 150 mM KCl, 5 mM perdeuterated DTT, 20 mM perdeuterated tris-AcOH (pH 6.2), and 10 μM EDTA. NMR titrations were carried out by adding unlabeled TAF_{1-140} dissolved in the same buffer. All NMR experiments were carried out at 300 K on a Bruker DMX500 spectrometer equipped with a *z*-shielded gradient triple resonance probe. Quadrature detection in the indirectly detected dimensions was achieved with the time-proportional phase incrementation (TPPI) method. The data were processed with the FELIX software (Biosym Technologies) with appropriate apodization, baseline correction, and zero-filling to yield real 2D 2K × 2K or 3D 512 × 256 × 128 matrices after reduction.
11. The coupling constants were obtained from the ^1H-^{15}N heteronuclear multiple-quantum coherence J-resolved (HMQC-J) spectrum [L. E. Kay and A. Bax, *J. Magn. Reson.* **86**, 110 (1990)].
12. The circular dichroism spectrum of $VP16_C$ alone at 6°C in buffer containing 50 mM phosphate buffer (pH 7.0) and 50 mM NaCl was characteristic for a random-coil structure.
13. The dissociation constant (K_D) of the $VP16_C$-TAF_{1-140} interaction was estimated to be $>10^{-4}$ M in NMR buffer containing 150 mM KCl. The limited solubility of TAF_{1-140} near the actual K_D range precluded accurate determination of K_D.
14. The sequential assignment of the HSQC cross-peaks was achieved by means of the following three-dimensional experiments: ^{15}N-edited nuclear Overhauser effect spectroscopy (NOESY)–HSQC; ^{15}N-edited total correlation spectroscopy (TOCSY)–HSQC; and HN(CO)CA, HNCA, and HCCH-TOCSY [M. Ikura, L. E. Kay, A. Bax, *Biochemistry* **29**, 4659 (1990); L. E. Kay, M. Ikura, R. Tschudin, A. Bax, *J. Magn. Reson.* **89**, 496 (1990); S. Grzesiek and A. Bax, *ibid.* **96**, 432 (1992); A. Bax, G. M. Clore, A. M. Gronenborn, *ibid.* **88**, 425 (1990); L. E. Kay, G. Xu, A. U. Singer, R. Muhandiram, J. D. Forman-Kay, *ibid.* **B101**, 333 (1993)].
15. Chemical shifts of the β protons were determined by NOESY-HSQC and TOCSY-HSQC experiments.
16. Protein-protein interaction assays were performed as in (*9*).
17. GAL4(1–147) and GAL4-VP16 fusions were expressed and purified essentially as described [D. I. Chasman, J. Leatherwood, M. Carey, M. Ptashne, R. Kornberg, *Mol. Cell. Biol.* **9**, 4746 (1989)]. All of the GAL4 fusion proteins had the expected mass, as determined by electrospray ionization mass spectroscopy. Activators (2 pmol) were preincubated with 100 ng of reporter construct pG_5BCAT and HeLa nuclear extract (50 μg) for 20 min at 20°C in a final volume of 30 μl in buffer containing 10 mM Hepes (pH 7.9), 7.5% glycerol, 1 mM DTT, 4 mM $MgCl_2$, 50 mM KCl, 10 mM ammonium sulfate, 1% polyethylene glycol, 0.2 mM PMSF, and bovine serum albumin (100 μg/ml). Transcription was initiated by adding 0.5 mM ribonucleotides and was then allowed to proceed for 30 min at 30°C. After primer extension [B. D. Dynlacht, T. Holey, R. Tjian, *Cell* **55**, 563 (1991)], the products were resolved on a 10% denaturing gel. The DNA binding activities of the GAL4 derivatives were verified by gel electrophoretic mobility shift assays.
18. A. P. Campbell and B. D. Sykes, *Annu. Rev. Biophys. Biomol. Struct.* **22**, 99 (1993).
19. $VP16_{469-485}$ was synthesized on an automated synthesizer and purified by high-performance liquid chromatography. The peptide was determined by electrospray ionization mass spectroscopy to have the expected molecular weight. The peptide was dissolved in 95% H_2O plus 5% ^2H_2O containing 150 mM KCl, 5 mM perdeuterated DTT, 20 mM perdeuterated tris-AcOH (pH 6.2), and 10 μM EDTA, and then the pH of the solution was adjusted to 6.2 by adding dilute KOH. The required amount of concentrated TAF_{1-140} was mixed with the peptide solution. The final concentrations of $VP16_{469-485}$ and TAF_{1-140} were 3 mM and 0.3 mM, respectively. The sequential assignment was obtained by TOCSY, double-quantum filtered correlation spectroscopy (DQFCOSY), and NOESY. In the NOESY spectra, 512 free induction decays were collected with a 5000-Hz sweep width and 2048 points in the F2 dimension, and the spectra were recorded at 300 K with mixing times of 100, 200, and 350 ms.
20. These observations lend credence to an early suggestion that acidic activation domains are α-helical when bound to their targets [E. Giniger and M. Ptashne, *Nature* **330**, 670 (1987)].
21. This perturbation is unlikely to result from indirect effects on the secondary structure of $VP16_C$, because Ala has a higher helical propensity than either Phe or Leu [P. Y. Chou and G. D. Fasman, *Adv. Enzymol. Relat. Areas Mol. Biol.* **47**, 45 (1978)].
22. S. K. Burley and R. G. Roeder, *Annu. Rev. Biochem.* **65**, 769 (1996).
23. M. L. Schmitz *et al.*, *J. Biol. Chem.* **269**, 25613 (1994).
24. P. H. Kussie *et al.*, *Science* **274**, 948 (1996).
25. Y. Lin, M. F. Carey, M. Ptashne, M. R. Green, *Cell* **54**, 659 (1988).
26. M. Zhang and H. J. Vogel, *Biochemistry* **33**, 1163 (1994).
27. We thank B. Dynlacht and J. Ross for helpful advice on transcription assays and S. Wolfe and P. Zhou for discussion about the NMR results. Supported in part by a grant from the Hoffman-La Roche Institute of Chemistry and Medicine and an NSF Presidential Young Investigator Award (G.L.V.); the Leukemia Society of America and the Naito Foundation (M.U.); and the Swiss National Foundation of Scientific Research (O.N.). The NMR spectrometer used in this work was purchased with funding from NSF (CHE93-12233).

18 March 1997; accepted 15 July 1997

Accelerated Aging and Nucleolar Fragmentation in Yeast *sgs1* Mutants

David A. Sinclair, Kevin Mills, Leonard Guarente

The *SGS1* gene of yeast encodes a DNA helicase with homology to the human *WRN* gene. Mutations in *WRN* result in Werner's syndrome, a disease with symptoms resembling premature aging. Mutation of *SGS1* is shown to cause premature aging in yeast mother cells on the basis of a shortened life-span and the aging-induced phenotypes of sterility and redistribution of the Sir3 silencing protein from telomeres to the nucleolus. Further, in old *sgs1* cells the nucleolus is enlarged and fragmented—changes that also occur in old wild-type cells. These findings suggest a conserved mechanism of cellular aging that may be related to nucleolar structure.

The *SGS1* gene of *Saccharomyces cerevisiae* is a member of the RecQ helicase family that includes human *BLM* (mutations in which cause Bloom's syndrome) (*1*), human *RECQL* (*2*), and *WRN* (*3*). Patients with Werner's syndrome contain two mutant alleles of *WRN* and display many symptoms of old age including graying and loss of hair, osteoporosis, cataracts, atherosclerosis, loss of skin elasticity, and a propensity for certain cancers (*4*). Cells isolated from patients with Werner's syndrome divide approximately half as many times in culture as those from normal individuals (*4*).

Department of Biology, Massachusetts Institute of Technology, Cambridge, MA 02139, USA.

Yeast cells lacking topoisomerase III activity (*top3*) are unable to unwind negatively supercoiled DNA efficiently and thus grow extremely slowly. Mutations in *SGS1* were first identified by their ability to suppress the slow-growth phenotype of *top3* strains (*5*); the Sgs1 protein was subsequently shown to interact physically with both topoisomerases II and III (*5–7*). *SGS1* is required for the fidelity of chromosome segregation and the suppression of recombination at the ribosomal DNA (rDNA) array and other loci (*5–7*).

Cell division in *S. cerevisiae* is asymmetric, giving rise to a large mother and a small daughter cell. Mother cells undergo, on average, a fixed number of cell divisions and

show characteristic changes with age, such as cell enlargement (8) and sterility (9). Age-related sterility is due to a loss of transcriptional silencing at the mating type loci *HMR***a** and *HML*α, and the resulting simultaneous expression of both **a** and α information (*10*). Old yeast cells also exhibit a loss of telomeric silencing (*11*). In young cells, silencing at *HM* loci and telomeres is mediated by the Sir2/3/4 protein complex (*12*, *13*). In addition, Sir2p silences marker genes inserted at rDNA (*14*) and suppresses recombination between rDNA repeats (*15*).

The genes *SIR2*, *SIR3*, and *SIR4*, as well as *UTH4*, are determinants of life-span in yeast (*16*). Null mutations in these genes shorten life-span (*17*), whereas overexpression of *UTH4* extends life-span. Life-span extension by the Sir complex is associated with a redistribution of these factors from telomeres (and *HM* loci) to the nucleolus in old cells—a process requiring *UTH4* (*16*, *18*).

We investigated the role, if any, of *SGS1* in yeast longevity. Life-span analysis of the wild-type *S. cerevisiae* W303-1A strain and an otherwise isogenic *sgs1* strain was carried out by micromanipulation until each mother ceased to divide. The average life-span of *sgs1* cells (9.5 divisions) was about 40% that of the wild-type strain (24.5 divisions) (Fig. 1A). The maximum life-span of the *sgs1* strain was similarly reduced (18 versus 40 divisions).

To determine whether the *sgs1* cells actually died from aging, rather than general sickness, we examined the age-specific phenotype of sterility as scored by their ability to respond to mating pheromone. In the *sgs1* mutant, young cells that had completed less than 50% of their life-span were almost always fertile (Fig. 2A). However, over 60% of cells in the last one-fifth of their life-span were sterile. This pattern, previously observed for wild-type cells, was due to a loss of transcriptional silencing at *HML*α (*10*). Deletion of *HML*α reduced the frequency of sterility in the *MAT***a** *sgs1* strain to almost zero (Fig. 2B).

Is sterility in yeast an aging-specific phenotype? We addressed this by examining two short-lived strains that were mutant for the transcriptional activator *HAP5* (*19*) or the coactivator *ADA1* (*20*). Although the two strains have significantly shortened life-spans (Fig. 1B), neither the *hap5* nor the *ada1* strains became sterile at a high frequency as they grew older (Fig. 2, C and D). Thus, sterility is an aging-specific phenotype that occurs prematurely in *sgs1* mutants.

Sgs1p was visualized by indirect immunofluorescence of fixed yeast cells (*16*). In >90% of cells, Sgs1p staining (green) was concentrated on one side of the nucleus (blue) (Fig. 3, A and B). Costaining cells for yeast Nop1p (red), an abundant nucleolar protein (*21*, *22*), demonstrated that the concentration of Sgs1p coincided with the nucleolus (Fig. 3C).

We then examined whether nucleolar changes occur during the life-span of *sgs1* cells. As observed for young wild-type cells (*21*), the nucleoli of young *sgs1* cells were well-defined structures occupying about 20% of the nucleus (Fig. 3D). In about 50% of old *sgs1* cells, the nucleolus was fragmented into several bodies that occupied a large fraction of the nucleus (Fig. 3E). In the remaining cells, a substantial enlargement of the structure was evident, which may be a prelude to fragmentation. In young wild-type cells expressing *SGS1* at high levels, a similar pattern of nucleolar fragmentation was observed (Fig. 3J), indicating that abundant Sgs1p may mimic the null phenotype by unbalancing the stoichiometry of an Sgs1p complex.

To determine whether fragmentation of the nucleolus was due to a scaling of a normal aging phenotype or was a consequence of the *sgs1* mutation per se, we examined the nucleoli of old wild-type cells. A substantial fraction (about 45%) of these had enlarged or fragmented nucleoli, similar to those in the *sgs1* cells (Fig. 3F). Fragmentation of the nucleolus in either young or old *ada1* cells was not observed (Fig. 3H).

Enlargement and fragmentation of the nucleolus may have been a response to an age-related reduction in protein synthesis. We therefore examined the nucleoli of starved young cells and found them to be ~25% the size of wild-type nucleoli and with a more rounded appearance (Fig. 3I). Hence, starvation is not a signal for nucleolar enlargement.

Compelling evidence that *sgs1* cells age prematurely would be the redistribution of Sir proteins to the nucleolus after only nine generations. In young *sgs1* cells, Sir3p staining showed characteristic telomere spots (*18*, *23*) (Fig. 4B). However, in old *sgs1* cells, Sir3p staining was predominantly nu-

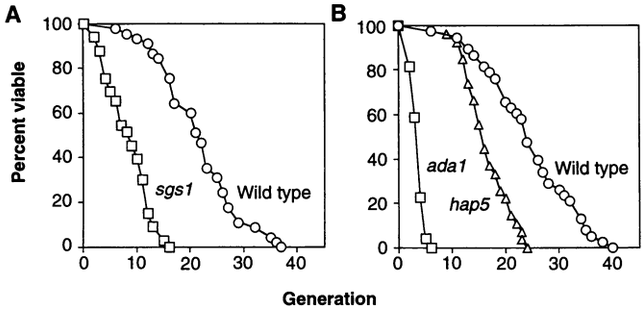

Fig. 1. Mutant *sgs1* cells have a short life-span. (**A** and **B**) Mortality curves of wild-type (W303-1A *MAT***a** *ade2-1 can1-100 his3-11,15 leu2-3,112 trp1-1 ura3-1*) and isogenic mutant derivatives *sgs1*::*HIS3*, *ada1*::*hisG*, and *hap5*::*hisG* were determined by the removal of daughters from virgin mothers by micromanipulation until senescence of the mother cell as determined by a cessation of cell division. Average life-spans (and sample sizes) were as follows: wild type, 24.5 (39); *sgs1*, 9.5 (30); *ada1*, 3.3 (23); and *hap5*, 16.6 (28).

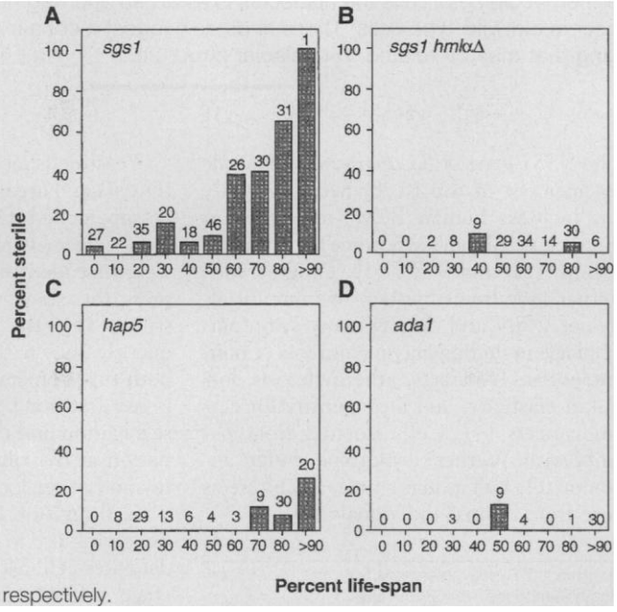

Fig. 2. Mutant *sgs1* cells age prematurely. (**A** to **D**) Cells of various ages were scored for their ability to undergo cell cycle arrest and schmooing in response to the yeast mating pheromone, α-factor. After 4 hours of α-factor challenge, cells were transferred to fresh medium to complete their life-span. Life-span is not affected by deletion of *HML* (*10*). Number of cells in each data set for each age group is shown above bar. Cells that failed to respond or divide after α-factor challenge were excluded from the data set. Disruption plasmids pCW9-1, pDM212 (*19*), and pADA1KO (*20*) were used to create *hml*α*Δ*::*LEU2*, *hap5*::*hisG*, and *ada1*::*hisG* strains, respectively.

cleolar. In old cells with fragmented nucleoli, Sir3p staining coincided with most or all nucleolar bodies (Fig. 4F).

Nucleolar enlargement and fragmentation could either represent a cause of aging or be a response to aging that promotes longevity. If fragmentation of the nucleolus is a longevity response in old cells, it might be caused by redistribution of the Sir complex to the nucleolus. Thus fragmentation would not occur in a *sir* null mutant. In old *sgs1 sir3* cells nucleolar fragmentation occurred at the same high level as in the *sgs1* single mutant (Fig. 3G), showing that the Sir complex does not cause fragmentation.

It was still possible that nucleolar enlargement and fragmentation were part of a longevity response, but did not require Sir protein redistribution. To test this possibility, we grew *SGS1* wild-type strains, which were either *SIR3* (wild type) or *sir3*, for 12 divisions and sorted them for old cells. At this age, many of the *sir3* cells are approaching senescence because of their shorter life-span. Nop1p staining showed that a substantial fraction of the nucleoli in the *sir3* mutant were either enlarged or fragmented (38% and 19%, respectively), a proportion much higher than in the age-matched wild type (12% and 6%, respectively) (Fig. 4, G and H). This finding suggests that the redistribution of the Sir complex to the nucleolus represses nucleolar fragmentation and promotes longevity.

Our data show that deletion of *SGS1* causes premature aging in yeast on the basis of three phenotypes: (i) the average life-span of *sgs1* cells is about 40% of wild type; (ii) *sgs1* cells prematurely assume the aging-associated sterility, whereas mutants for other yeast genes either do not display a shorter life-span or do not exhibit the age-specific phenotype of sterility; and (iii) the Sir protein silencing complex redistributes from telomeres to the nucleolus in old *sgs1* cells, as observed in old wild-type cells.

We observed a profound enlargement and fragmentation of the nucleolus in old *sgs1* and wild-type cells. These fragments may result from a breakdown of nucleolar architecture or result from the inherent instability of the rDNA itself. We favor the latter hypothesis. Further, the nucleolar fragments were often arrayed in an orderly series around the periphery of the nucleolus, perhaps reflecting a mechanism that promotes assymetric segregation of the fragments to mother cells.

We cannot rule out the possibility that nucleolar enlargement and fragmentation are simply markers of aging. However, we do not favor this view because (i) an independent study has indicated a central role for the nucleolus in determining life-span (*16*), and (ii) the localization of Sgs1p in the nucleolus suggests that a nucleolar defect resulting from its absence may be a direct cause of premature aging.

The data herein indicate that nucleolar

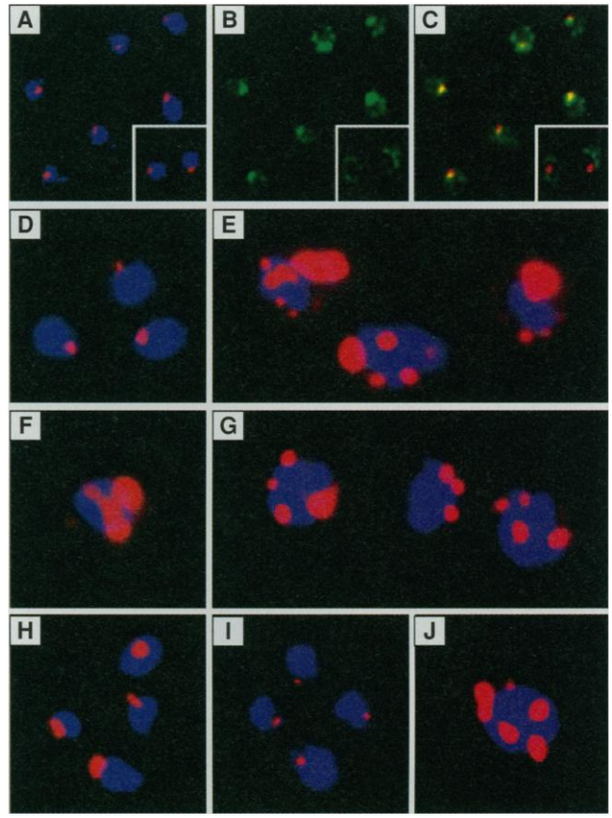

Fig. 3. Nucleolar localization of Sgs1p and nucleolar fragmentation in old cells. *Escherichia coli* recombinant 6-histidine–tagged Sgs1p (amino acids 1071 to 1447) was affinity-purified with Ni-NTA agarose (*28*). Immunoglobulin Y (IgY), which recognized 0.1 ng of Sgs1p, was affinity-purified from chicken serum with the use of recombinant Sgs1p. (**A**) Young wild-type cells stained for DNA with 4′,6′-diamidino-2-phenylindole (DAPI) (blue) and yeast fibrillarin with a monoclonal antibody to Nop1p (*22*) and Cy3-conjugated goat antibody to mouse (anti-mouse) IgG (red). (**B**) Sgs1p stained with sheep fluorescein isothiocyanate (FITC)–conjugated IgG against chicken anti-Sgs1p (green). (**C**) Merged image of Sgs1p and Nop1p (overlap is yellow). *sgs1* mutant strains treated identically (insets A to C) showed only background staining. (**D** to **J**) Cells were stained with anti-Nop1p (red) and DAPI (blue) (*18*): (D) young *sgs1* cells; (E) old *sgs1* cells [average bud scar count (ABSC) of magnetic sort ± SD: 9 ± 2]; (F) old wild-type cells (ABSC = 26 ± 3); (G) old *sgs1 sir3::URA3* cells (ABSC = 8 ± 2); (H) old *ada1* cells (ABSC = 2 ± 1); (I) starved wild-type cells; and (J) cells overexpressing Sgs1p from an inducible GAL-promoter (*29*). *SIR3* was disrupted with pDM42. Starved cells were obtained by growing first in yeast extract–bactopeptone–glucose to stationary phase, then in 2.4 g/liter yeast nitrogen base without amino acids for 12 hours.

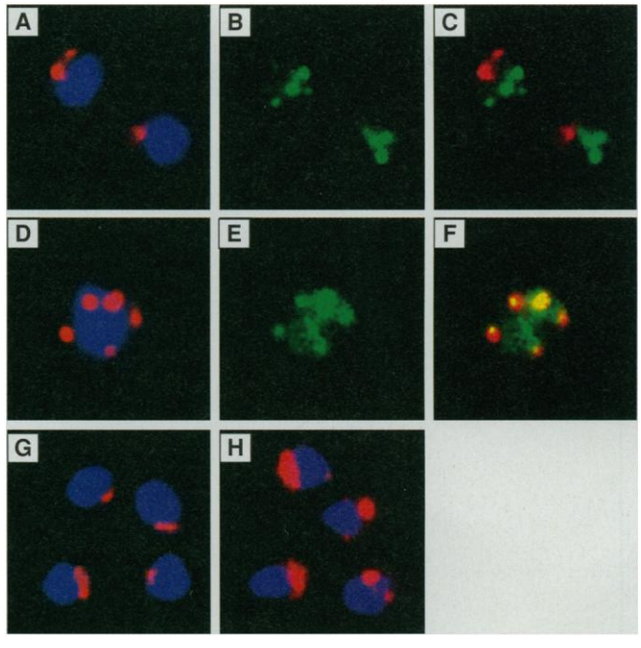

Fig. 4. Sir3p localized to nucleolar fragments of old *sgs1* cells. Old *sgs1* cells were obtained by magnetic sorting (ABSC ± SD = 9 ± 2) and stained as in Fig. 3. Nop1p is shown in red (A, C, D, F); DNA is in blue (A and D); Sir3p was visualized with FITC-conjugated goat anti-rabbit IgG (green) (B, C, E, F). Overlap of Sir3p and Nop1p staining is shown in yellow. (**A** to **C**) Young *sgs1* cells. (**D** to **F**) Old *sgs1* cells. (**G** to **H**) Twelve-generation old wild-type and *sir3* cells stained for DNA (blue) and Nop1p (red). (G) Wild-type cells. (H) *sir3* mutant cells. Proportion of cells with small, large, or fragmented nucleoli (percent): wild type (82, 12, 6); *sir3* (43, 38, 19).

enlargement and fragmentation represent a cause of yeast aging, and that these changes are delayed by the redistribution of Sir proteins to the nucleolus. The similar effect of the related *SGS1* and *WRN* genes on yeast and human aging along with age-associated changes in rDNA content reported for several mammalian species (*24*, *25*) suggest that a common mechanism may underlie aging in eukaryotes.

REFERENCES AND NOTES

1. N. A. Ellis *et al.*, *Cell* **83**, 655 (1995).
2. K. L. Puranam and P. J. Blackshear, *J. Biol. Chem.* **269**, 29838 (1994); M. Seki *et al.*, *Nucleic Acids Res.* **22**, 4566 (1994).
3. C.-E. Yu *et al. Science* **272**, 258 (1996).
4. D. Salk, K. Au, H. Hoehn, M. R. Stenchever, G. M. Martin, *Cytogenet. Cell Genet.* **30**, 108 (1981); G. M. Martin, *Adv. Exp. Med. Biol.* **190**, 161 (1985).
5. S. Gangloff, J. P. McDonald, C. Bendixen, L. Arthur, R. Rothstein, *Mol. Cell. Biol.* **14**, 8391 (1994).
6. P. W. Watt, E. J. Louis, R. H. Borts, I. D. Hickson, *Cell* **81**, 253 (1995).
7. P. M. Watt, I. Hickson, R. H. Borts, E. J. Louis, *Genetics* **144**, 935 (1996).
8. R. K. Mortimer and J. R. Johnson, *Nature* **183**, 1751 (1959).
9. I. Müller, *J. Microbiol. Serol.* **51**, 1 (1985).
10. T. Smeal, J. Claus, B. Kennedy, F. Cole, L. Guarente, *Cell* **84**, 633 (1996).
11. S. Kim, B. Villeponteau, S. M. Jazwinski, *Biochim. Biophys. Res. Commun.* **219**, 370 (1996).
12. A. J. Klar, J. N. Strathern, J. R. Broach, J. B. Hicks, *Nature* **289**, 239 (1981); J. M. Ivy, A. J. S. Klar, J. B. Hicks, *Mol. Cell. Biol.* **6**, 688 (1986); J. Rine and I. Herskowitz, *Genetics* **116**, 9 (1987).
13. D. E. Gottschling, O. M. Aparicio, B. L. Billington, V. Zakian, *Cell* **63**, 751 (1990); O. M. Aparicio, B. L. Billington, D. E. Gottschling, *ibid.* **66**, 1279 (1991).
14. M. Bryk *et al.*, *Genes Dev.* **11**, 255 (1997); J. S. Smith and J. D. Boeke, *ibid.*, p. 241.
15 S. Gottleib and R. E. Esposito, *Cell* **56**, 771 (1989).
16. B. K. Kennedy *et al.*, *ibid.* **89**, 381 (1997).
17. B. K. Kennedy, N. R. Austriaco, J. Zhang, L. Guarente, *ibid.* **80**, 485 (1995).
18. M. Gotta *et al.*, *EMBO J.* **16**, 3243 (1997).
19. D. S. McNabb, Y. Xing, L. Guarente, *Genes Dev.* **9**, 47 (1995).
20. J. Horiuchi, N. Silverman, B. Piña, G. A. Marcus, L. Guarente, *Mol. Cell. Biol.* **17**, 3220 (1997).
21. R. Henriquez, G. Blobel, J. P. Aris, *J. Biol. Chem.* **265**, 2209 (1990).
22. D. Tollervey, H. Lehtonen, M. Carmo-Fonseca, E. C. Hurt, *EMBO J.* **10**, 573 (1997).
23. F. Palladino *et al.*, *Cell* **75**, 543 (1993).
24. B. Strehler, *Exp. Gerontol.* **21**, 283 (1986); J. Halle, S. Müller, A. Simm, G. Adam, *Eur. J. Cell. Biol.*, in press.
25. F. B. Adamstone and A. B. Taylor, *J. Morphol.* **154**, 459 (1979); F. Puvion-Dutilleul and A. Macieira-Coelho, *Exp. Cell Res.* **138**, 423 (1983); M. E. Weintein and A. B. Mukherjee, *Mech. Ageing. Dev.* **42**, 215 (1988).
26. F. W. Studier, *J. Mol. Biol.* **189**, 113 (1991).
27. P. K. Foreman and R. W. Davis, *Gene* **144**, 63 (1994).
28. The region encoding the COOH-terminus of Sgs1 was amplified by the polymerase chain reaction (PCR) (from +3208 to +4344) with oligonucleotides GGGGGGGATCCAATTGTAGAAATAGCGCCAACG and GGGGGGAGCTCTCACTTTCTTCCTCTGTAGTGA. The product ligated to pET-28a(+) (Novagen) between Bam HI and Sac I to create pET28N-SGS1. BL21(DE3) cells (*26*) were transformed with pET28N-SGS1 and grown in 2 liters of complete medium to an absorbance at 600 nm of 1. Expression was induced with 1 mM isopropyl-β-D-thiogalactopyranoside for 4 hours. Sgs1p was purified with Ni–nitrilotriacetic acid (NTA) agarose under standard conditions.
29. *SGS1* was amplified by the PCR with oligonucleotides GGGGGGGATCCAGTGACGAAGCCGTCACATAACTTA and GGGGGGCGGCCGCTTATCACTTTCTTCCTCTGTAGTGACC for insertion downstream of the galactose-inducible promoter of yCPlF15 (*27*). Overexpression of *GALp-SGS1* was induced by growing for 4 hours in YPGal (10 g/liter yeast extract, 20 g/liter bactopeptone, 2 g/liter galactose), and confirmed by protein immunoblot analysis.

30. We thank S. Gasser and E. Hurt for antibodies to Sir3p and Nop1p; J. Broach (pDM42), J. Haber (pCW9-1), B. Johnson, D. McNabb, J. Horiuchi, and S. Mah for plasmids and advice; Y.-H. Tu for CELLScan imaging assistance (NIH S10RR917-01); and the Kaiser lab for their Axioscope. Supported by the Helen Hay Whitney Foundation (D.A.S.) and by a National Institutes of Health predoctoral training grant (K.M.). The Guarente lab is supported by a National Institutes of Health grant (AG11119).

8 May 1997; accepted 9 July 1997